Enabling Silicon Anodes with Novel Isosorbide-Based Electrolytes

*Noah M. Johnson, Zhenzhen Yang, Minkyu Kim, Dong-Joo Yoo, Qian Liu, and Zhengcheng Zhang**

Chemical Sciences and Engineering Division,

Argonne National Laboratory,

9700 S. Cass Ave., Lemont, IL 60439, USA

*zzhang@anl.gov

Abstract

Silicon is seen as one of the most promising anode candidates for next generation lithium-ion batteries, due to its high theoretical capacity and energy density. However, many technical barriers remain to its implementation, due to its high chemical/electrochemical reactivities with standard electrolytes and incomplete passivation from large volume changes. Herein, we report an isosorbide dimethyl ether (IDE)-based electrolyte, which exhibits much improved stability as evidenced by long cycle life and calendar life. Analysis of the cycled silicon surface shows minimal decomposition of organic species from IDE solvent, confirming the electrolyte maintains a limited chemical reactivity with nucleophilic lithiated silicon (Li_xSi). This research opens up new avenues for designing new electrolytes which could ultimately enable the practical application of silicon anodes.

Table of Content

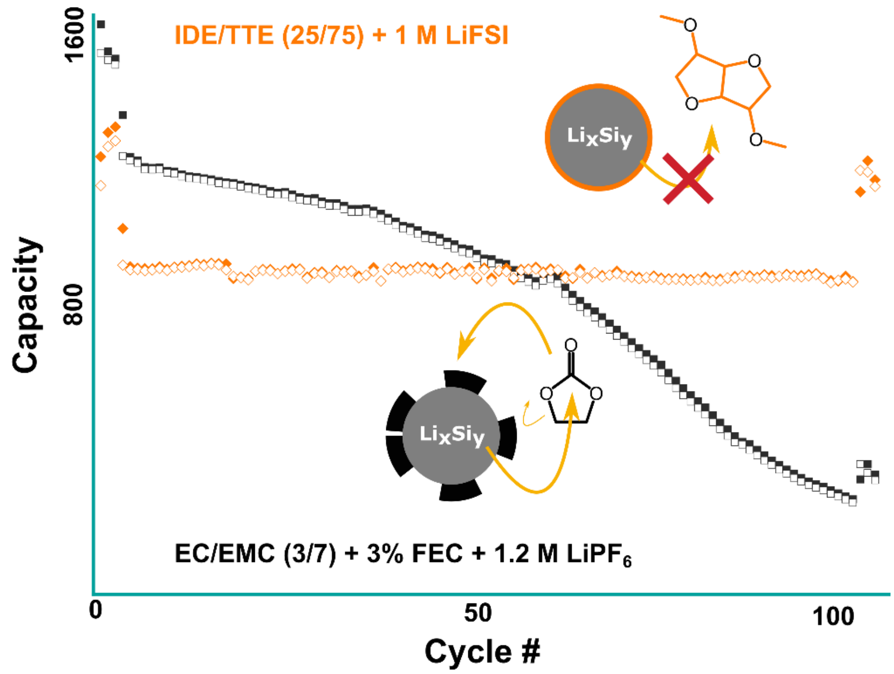

Lithium-ion batteries (LIBs) are one the of the most prominent forms of electrochemical energy storage. Their high energy density, long lifespan, and broad voltage range has enabled applications in technology ranging from toys to satellites. However, as the world transitions to a greener ecosystem, the range of technologies that utilize electrochemical energy storage will need to increase, and the current LIBs are insufficient to the task.[1-3]

One promising new candidate for LIBs is the silicon (Si) anode and its successful application in LIBs will lead to wide adoption of electric vehicles. Si has a much higher specific capacity (3579 mAh/g) than the current state-of-the-art anode, graphite (372 mAh/g).[4, 5] As well, Si is more resistant to lithium dendrite formation, and is a very common element in the earth's crust. However, it suffers from a severe weakness in a lack of surface passivation and the kinetic stability during the repeated lithiation/delithiation.[5] While graphite can reliably form a stable solid-electrolyte-interphase (SEI) that prevents future reactivity of electrolyte solvent with the lithiated graphite, Si experiences continual reactivity without SEI formation and surface passivation. This is due to a 300% volume expansion and contraction during the lithiation and delithiation process, which disrupts the surface of silicon particles, an instability of the electrolyte decomposition products, as well as the chemical reactivity of the electrolyte from the highly charged Si^{4-} in lithiated silicon.[4, 6-10] Analysis of silicon nanowires with cryo-TEM has also shown that even minimal passivation may be short-lived[11]. The initial cycles show a distinct surface layer formed on top of the silicon, as would be expected from a typical graphite SEI. However as cycling continues, this interface is progressively enfolded, bringing the decomposed electrolyte products into the interior of the nanowire. This process will break the silicon into smaller nanodomains, some of which will be electrically disconnected and unable to be lithiated. As well, it will expose more silicon surfaces to the electrolyte once again, continuing the decomposition of the electrolyte. This raises the question of whether silicon can ever be fully passivated.

One method that's been explored for stabilizing silicon is modifying the surface of the silicon *ex-situ*. The interface of the silicon can be modified directly, using precise methods such as chemical vapor deposition (CVD), atomic layer deposition (ALD), acetylene gas reduction, or solution chemistry to create a monolayer of passivating materials on the surface of the silicon nanoparticles.[12-16] Nano-engineering has also been used to embed silicon nanoparticles in a passivating carbon framework, such as reduced acetylene gas, a core-shell conformation, or a bulk coating of inexpensive pitch.[17, 18] However, *ex-situ* modification tends to greatly increase the cost of the active materials, and can decrease overall silicon utilization.

A more practical alternative would be an electrolyte that can form a passivating SEI, and many attempts have been made in this direction. One popular route is the use of small amounts of sacrificial additives that can prevent further reaction of the silicon surface with the electrolyte. Two of the most common in this category are fluoroethylene carbonate (FEC) and vinylene carbonate (VC), which have been used to great effect to improve the cycle and calendar life of silicon-based anodes. Unfortunately, their performance is proportional to the concentration of these materials, as they are continuously consumed during operation.[19-21] Many other additives have attempted to achieve similar effectiveness, including lithium difluoro(oxalate)borate (LiDFOB), alkoxy-substituted silanes, succinic anhydride, and isocyanates.[22-25] However, none have managed to stabilize silicon under practical conditions.

A potential reason for this instability is that the electrolyte solvent itself is incompatible with lithiated silicon (Li_xSi, x=1-4). Li_xSi is a nucleophile and tends to attack the nucleophilic carbon of the carbonyl from the carbonates leading to decomposition of the electrolyte. Attempts to create a new solvent system that is less or non-reactive tend to be rarer, but excellent results have been seen with a few systems, even in the absence of additives. For example, an electrolyte using tetrahydrofuran (THF) and 2-methyltetrahydrofuran (mTHF) as the electrolyte solvent was able to show excellent cycling performance on microsized silicon half cells, with Coulombic efficiencies (CE) over 99.9%.[26] Other ether-based systems have seen similarly good performance, using cyclic ethers such as 1,3-dioxolane (DOL) or linear ethers such as dimethoxyethane (DME).[27, 28] However, these ether based solvent systems rely on saturating the ethers with lithium ions, through elevated salt concentrations or dilution with non-coordinating solvents (localized high concentration electrolyte). This limits the new electrolyte design space, when compared to a stable non-reactive solvent. Ionic liquids have also seen excellent results, with piperidinium bis(fluorosulfonyl)imides stabilizing Si/NMC full cells up to 4.7 V.[29, 30] These solvents unfortunately tend to be prohibitively expensive, along with having severe C-rate limitations and poor wetting capability.

We undertook to resolve these issues by using an ether solvent containing a bicyclic ring that has low reactivity to silicon. This would render the volume expansion of silicon insignificant, as the lithiated silicon surface would still be relatively stable to the solvent system. We chose isosorbide dimethyl ether (IDE) as an example, which also has the benefits of being a green material, inexpensive, commercially available, non-toxic, and non-flammable. We hypothesized that the conformation of this molecule, as seen in **Figure 1** would allow encapsulation of lithium ions, giving high lithium salt solubility. Modeling work on cyclic carbonates has also indicated that interaction with the silicon surface is very sensitive to the chemical structure, with the electronegative atoms interacting directly with the silicon surface.[31, 32] The shape of IDE molecule would make this alignment difficult, therefore blocking or decreasing the rate of any reaction with the surface.

In this paper, we demonstrate the effectiveness of the non-reactive IDE-based electrolytes in an LFP/silicon electrochemical couple by very low leakage currents during the potentiostatic hold when compared to standard carbonate-based electrolytes and greatly enhanced cycle life and calendar life.

IDE Solo Electrolytes – 1 M $LiPF_6$ IDE and 1 M LiFSI IDE

For the purposes of this study, $LiFePO_4$ (LFP) was chosen as the positive electrode, with a loading such that the n:p ratio of the cell is less than 1. The flat voltage profile allows the silicon negative electrode to be fully lithiated to ~120 mV, and the low upper-cutoff voltage (UCV) of 3.35 V and high stability of the LFP will allow an assumption that any degradation is from reactions with the silicon itself. This contrasts with a lithium-metal counter electrode, which introduces its own reactivity. Due to this full utilization of the silicon, discharge capacities are given relative to the amount of silicon in the electrode.

Early in the first cycle of LFP/Si cell, electrolyte components susceptible to reduction will react with the Si negative electrode, forming a solid-electrolyte interphase (SEI) that insulates the electrolyte from further reactions. In **Figure 2a**, a differential capacity plot (*dQ/dV*) of this early phase is shown, highlighting the electrochemical reduction reactions that contribute to the formation of this interphase. For the baseline electrolyte GenF (a mixture of ethylene carbonate (EC) and ethyl methyl carbonate (EMC) dissolved with 1.2 M $LiPF_6$ + 3% (w/w) of fluoroethylene carbonate (FEC)), these signals are easily visible. There are two main peaks, a sharp signal at 2.43 V, and a broader peak at 1.93 V, both of which have previously been assessed to correspond to the reduction of FEC.[33] No other signals are visible, as the FEC reduces prior to other components of the electrolyte. In contrast, two electrolytes based on IDE show very little in the way of SEI-forming species. The *dQ/dV* shows only a shoulder starting at 2.50 V, which only corresponds to the beginning of lithiation process of silicon anode.

A voltage profile for the entire 1st cycle can be seen in **Figure S1**. The charging profile is a slowly flattening plateau, beginning around 3.0 V and continuing to flatten until reaching the UCV. The discharge profile is more well-defined with a broad slope beginning at 3.15 V, and a flatter plateau beginning at 2.95 V. The baseline electrolyte GenF maintained a 1st cycle discharge capacity of 1511 mAh/g_{Si}, and a 1st cycle Coulombic efficiency (CE) of 69.8%. This is similar to what can be obtained from a lithium/Si half cell in the equivalent voltage range, further supporting the efficacy of using LFP as a positive electrode. The voltage profiles for the IDE/$LiPF_6$ and IDE/LiFSI electrolytes show a significant overpotential relative to GenF, which is particularly evident during the discharge step. Here, the overpotential is large enough to miss the second plateau seen in the GenF electrolyte, leading to a discharge capacity of 812 mAh/g_{Si} and CE of 62.6% for 1M $LiPF_6$, and 1133 mAh/g_{Si} and 69.3% for 1M LiFSI, respectively.

A difference in the electrolytes was visible during cell assembly, as the IDE electrolytes, particularly that using $LiPF_6$ as the salt, were significantly more viscous than the GenF electrolyte. Their wetting properties were also much worse and didn't improve upon use of glass-fiber separators. Such a high viscosity would be expected to cause a low conductivity, which might lead to decreased performance relative to GenF upon increasing the current density. For this reason, we performed a cycle life test at C/3 to test the cycling stability of the three electrolytes at higher current densities (**Figure 2b**).

After three C/10 cycles, GenF has a discharge capacity of 1645 mAh/g_{Si}, which drops to 1362 mAh/g_{Si} when the cycling rate is increased to C/3. The discharge capacity and CE then slowly fall, with the decline accelerating around cycle 60. By the 100th cycle, the discharge capacity has declined to 284 mAh/g_{Si}, and the CE has dropped to 96.2%. Returning to C/10 barely increases the discharge capacity, establishing that the decline was due to lithium inventory consumption caused by the reaction of the electrolyte with the continually expanding and contracting silicon surface.

The IDE electrolytes show very different behavior. IDE + 1 M LiFSI has a discharge capacity of 1139 mAh/g_{Si} after three C/10 cycles, dropping to 696 mAh/g_{Si} when increasing to C/3. This is consistent with the high viscosity of the electrolyte, which will respond more severely to higher C-rates. Unfortunately, an external temperature change around cycle 68th artificially increased the discharge capacity, masking what the final outcome would be. What can be noted is the overall steady performance, and the return to nearly the original discharge capacity upon returning to C/10 cycling. This supports a conclusion that IDE is relatively stable to the silicon surface. This can also be seen in the elevated CE, which averages to 99.7% over the last 50 cycles, compared to GenF at 97.3%. A similar set of results can be seen for IDE + 1 M $LiPF_6$, which exhibits a more severe capacity drop to 227 mAh/g_{Si} due to its higher viscosity, but still shows a high capacity retention of 93.6%, and an average CE of 99.9%.

From this set of results, it can be concluded that IDE does show a very high stability to lithiated silicon, based on the extremely high capacity retention and Coulombic efficiency relative to GenF. However, the capacity at higher current densities is impractically low, due to the high viscosity of the IDE solo electrolyte and will need to be improved to make a useful battery system.

TTE-Diluted IDE Electrolyte

In order to reduce the viscosity of IDE-based electrolytes, we opted to take the strategy of addition of low viscosity cosolvents. A number of classes were investigated, including fluorinated carbonates, esters, nitriles, ethers, amides, and ureas. Although viscosity was improved with these cosolvents, most ended up with deterioration in performance due to parasitic interactions with the silicon anode. As an example, using DME as a cosolvent decreased the stability of the electrolyte in direct proportion to its concentration. Capacity retention fell from 85.8% for a 75/25 (v/v) ratio of IDE/DME down to 56.4% for a 25/75 ratio. Similarly, CE fell from 99.5% to 98.6%. Together, these results indicate that despite DME performing well in certain electrolyte compositions including localized high concentration electrolytes[28], it is itself unstable to lithiated silicon. This would explain the increasingly poor performance as more DME is added into the system. As IDE's improved performance is due to a high stability to lithiated silicon – in contrast to efficient passivation – any cosolvent will be free to react with the silicon surface normally, and usually detrimentally.

Eventually, we discovered that 1,1,1-trifluoroethyl-1,1,2,2-tetrafluoropropyl ether (TTE) was itself stable to the silicon, while still leading to a significant decrease in viscosity. This decline in viscosity is nearly linear with increasing amounts of TTE (**Figure S2**), eventually declining to 8.4 cP at an IDE/TTE ratio of 25/75 in volume, which is near the saturation point with 1 M LiFSI. This value is still higher than the viscosity of GenF at 4.2 cP, so some decline in discharge capacity at higher C-rates is expected.

Density Functional Theory (DFT) calculations show that IDE has a binding energy to the Li^+ which is similar to ethylene carbonate (EC), but significantly stronger than TTE (**Table S1**), indicating the solvation sheath with Li^+ would be expected to contain mainly IDE, while TTE is non-solvating and solely serving to decrease viscosity. The lowest unoccupied molecular orbital (LUMO) for IDE is also 0.2 eV higher in energy than TTE or EC, which would make it less likely to be reduced on the silicon surface. This is in line with our design strategy, where our solvent system is supposed to have a low reactivity with silicon during repeated cycling.

The cycling performance with different ratios of IDE/TTE are shown in **Figure 3**. Decreasing the viscosity with added TTE leads to a predictable increase in starting discharge capacity when compared to the highly viscous IDE solo electrolytes. At C/3 this increase is nearly linear, rising from the 696 mAh/g_{Si} for IDE alone to 1023 mAh/g_{Si} for IDE/TTE (25/75), while the CE remains constant at 99.7%. While this discharge capacity is still well short of GenF, the increased stability of IDE more than compensates after 100 cycles, when the IDE/TTE (25/75) has a capacity retention of 90%, compared to GenF at 22%. This stable capacity retention and CE for all IDE/TTE electrolytes indicates that the TTE isn't changing the stability of the electrolyte, as is seen for LHCEs.[28, 34] Instead, the decreased viscosity caused by the increasing proportion of TTE improves conductivity, thus allowing the electrolyte to utilize more of the silicon active material.

The impact of non-reactive IDE/TTE can also be seen by looking at the difference between the average charging voltage and the average discharging voltage (ΔV). This value will increase proportionally to the internal resistance of the cell,[35] as the resistance will cause the voltage profiles to shift in the direction of current flow. In a perfect scenario this value will remain constant throughout the aging protocol. Unfortunately, in practice it generally increases - decomposition from the electrolyte thickens interphases, active materials degrade, electrical contact is broken, etc.

The effect of this can be clearly seen in **Figure S3.** GenF starts the C/3 cycling at a relatively low ΔV of 267 mV, which then slowly rises over the course of the experiment. This is proportional to the fall in capacity in **Figure 3**. The rise rapidly accelerates around cycle 60, coincident with the increasing drop in capacity, and ends cycling with a ΔV of 323 mV. By contrast, the IDE/TTE electrolyte start at higher values of ΔV, likely due to their still higher viscosity. There is a general trend of decreasing viscosity leading to lower starting values of ΔV, ranging from 426 mV for 100% IDE to 336 mV for IDE/TTE (25/75). However, all the IDE-based electrolytes change very little in ΔV, outside of the shifts from the previously mentioned external temperature changes. This indicates that there is very little degradation occurring in the systems with an IDE/TTE electrolyte, regardless of the ever-changing surface that is characteristic of the silicon anode.

While ΔV is a very useful metric for tracking overall cell resistance, it is not helpful for determining what factors are contributing to any changes. For this, we turn to electrochemical impedance spectroscopy (EIS), the results of which can be seen in **Figure 4a**. Here, GenF is compared only to IDE/TTE (25/75) for the sake of clarity. After formation cycles, the most obvious difference between the two EIS spectra is that the IDE/TTE cell has a much larger bulk impedance, causing the curve to be shifted to the right. The interfacial impedance (R_{SEI}) assigned to the high-frequency semicircle, of the two cells are nearly identical, 10.3 Ω for GenF and 12.3 Ω for IDE/TTE. The charge-transfer impedances (R_{CT}), assigned to the middle-frequency semicircle, is somewhat higher for IDE/TTE, at 9.9 Ω compared to 4.8 Ω. However, this is dwarfed by the bulk impedance (R_0), which increases from 2.7 Ω for GenF to 23.8 Ω for IDE/TTE. This indicates that at the beginning of cycling, the cell resistance will be dominated by R_0, which includes the properties of electrolyte.

After the aging protocol has completed, the EIS spectra has changed. While the bulk impedances haven't changed by much, the interfacial and charge transfer resistances have drastically increased for the cell with the GenF electrolyte. Here, the interfacial impedance has increased to 82.2 Ω, and the charge-transfer impedance has increased to 196.9 Ω. This large increase in impedance matches what is observed in **Figure S3**, as the ΔV of GenF increased over the course of the experiment. Also as was observed, the IDE/TTE changed far less relatively, with interfacial impedance increasing to 21.7 Ω and charge-transfer impedance increasing to 35.0 Ω. This supports the conclusion that IDE/TTE has a low reactivity to the silicon surface.

IDE/TTE calendar life

One of the most challenging barriers for silicon anodes is poor calendar life. While cycling can be optimized to enable large cycle numbers and high energy density and specific capacity, calendar life remains far short of what would be expected in a practical battery system[36-38]. One way to approximate relative calendar life is to measure leakage currents against a flat voltage profile, such as that seen in LFP. The flat voltage profile will ensure that any measured current is relate to reactions at the anode, where voltage changes can be measured. A higher baseline leakage current will indicate an electrolyte fundamentally unstable to silicon, and therefore one that will have a short calendar life.

The results of this test are shown in **Figure 4b**. During the initial stage, the current of the IDE/TTE electrolyte is much higher than the GenF. However, this stage tends to be dominated by reversible lithiation of the silicon anode, which is anticipated to be slower in the higher viscosity electrolyte system. This is bolstered by the nearly exponential decline (linear on the log scale), indicating that the current is dominated by a single electrochemical process. The current from the carbonate electrolyte has leveled off after ~25 hours, indicating that reversible lithiation has completed, and the irreversible electrolyte consumption is now the dominant process. It continues to slowly decrease until ~300 hours, when the excess lithium has been entirely consumed. By contrast, the IDE/TTE electrolyte continues declining linearly until it reaches the detection limits of the instrument. This would indicate that the IDE/TTE electrolyte is stable to the lithiated silicon at the chosen potential in a way that the carbonate electrolyte cannot achieve.

Effect of Hydrofluoroether (HFE) Diluents

Now that an effective electrolyte had been discovered for silicon, we endeavored to see whether the IDE/TTE pairing was unique. To determine this, we tested a variety of other HFEs, including bis(2,2,2-

trifluorethyl)ether (**BTFE**), 1,1,2,2-tetrafluoroethyl-2,2,2-trifluoroethyl ether (**TFTFE**), and 1,2-bis(2,2,3,3-tetrafluoroethoxy)ethane (**TFEE**). These HFE's were chosen to explore the effect of fluorinated structure on any interaction with the silicon surface. TFTFE includes a trifluoromethyl functionality, while maintaining the O-CH_2-CF_x group which may be reactive to the silicon surface. TFEE abandons this functionality entirely, while changing to a glyme structure that may participate in Li^+ solvation. BTFE, on the other hand, abandons the -CF_2H functionality entirely. The electrolytes were all made in a 50/50 ratio with IDE, as the interest is in their stability to silicon, not their viscosity.

The *dQ/dV* for the first charge of the cells shows very little difference between the electrolytes in terms of their SEI forming peaks, particularly when compared to GenF (**Figure 5a**)**.** This implies that regardless of their structural conformation, none of the HFEs react with the silicon surface to form a discrete peak in the *dQ/dV*. The similarity continues, as all IDE/HFE electrolytes have the same shoulder starting around 2.50V, and nearly identical curves up through the first lithiation event.

Upon beginning C/3 cycling, there is a difference in conductivity between the electrolytes, as would be expected (**Figure 5b**). This can be easily seen from the starting discharge capacity, which is 804 mAh/g_{Si} for TFEE, 885 mAh/g_{Si} for BTFE, and 479 mAh/g_{Si} for TFTFE. The order of conductivity, presumably caused by differences in viscosity, therefore seems to be BTFE>TFEE>>TFTFE. Despite these starting differences, all the electrolytes ended up with very similar performance with regards to capacity retention and CE, indicating that using IDE as a lithium-coordinating solvent is generally compatible with any co-solvent that has stability with silicon.

Silicon Surface Analysis

X-ray Photoelectron Spectroscopy (XPS) was employed to view the stability of the IDE/TTE electrolyte with silicon (**Figure 6**). When compared to the pristine Si anode, the electrode cycled in GenF shows a few key differences in the C1s spectra. The first is the disappearance of the peak appearing at 283.4 eV, which is associated with the sp^2 C-C bond in carbon allotropes such as graphite, carbon nanofibers, or in this case, conductive carbon black.[39, 40] The second is a general enrichment in oxidized carbon species - with peaks around 286 eV, 288 eV, and 289-290 eV - relative to the hydrocarbon peak, referenced at 285 eV. This is a result of the carbonate-based solvent breaking down into a mixture of organic lithium carbonates at lower voltages.[41] In contrast, the IDE/TTE electrolyte shows very low prevalence of these species, indicating the presence of minimal decomposed organic materials from the IDE/TTE solvents. For both GenF and IDE/TTE electrolytes, the O1s peak has a similar ratio of C-O to C=O species, which suggests that any organic species present are similar in chemical structure.

The F1s spectra also indicate minimal decomposition of organic materials. The pristine Si electrode has a minimal number of fluorine-containing species, mainly represented by organic fluorides near 687 eV. In contrast, the electrode cycled in GenF shows a majority contribution from the LiF, with significant amounts of organic fluorides originating from either C-F bond in decomposed FEC, or fluorophosphates originating from $LiPF_6$. However, the Li1s doesn't indicate the presence of any lithium species besides LiF, fluorophosphate species are a minimal contributor to the decomposition on silicon.[40, 42] IDE/TTE has negligible amounts of organic fluorides, and instead shows a very strong LiF peak, further supporting a conclusion of minimal organic decomposition of the new electrolyte.

This increase in LiF relative to organic components has also been seen in other fluorinated and ether-based electrolyte systems, such as FEC,[43] tetrahydrofuran (THF),[26] and glyme-based solvents.[28] While LiF is an important component of a robust SEI, and is necessary to prevent electron tunneling from causing further electrolyte decomposition,[44] it is also physically brittle and weak, a property which would be detrimental to an expanding surface such as silicon.[45] This makes the value of LiF to a silicon SEI suspect, and is here more likely a sign of a stable electrolyte.

Improved Safety of IDE Electrolyte

One of the dangers in using carbonate solvents is their high flammability. As an example, ethyl methyl carbonate (EMC) has a flash point of 23°C at room temperature, which makes these solvents a hazard when combined with the energy-releasing potential of Li^0 when exposed to air. By comparison, IDE has a flash point of 110°C, which makes it a non-combustible liquid. As well, TTE and its HFE analogs have been shown to have flame-extinguishing properties, and it would be hypothesized that such an IDE/TTE combination would have enhanced safety of the battery. **Figure S4** shows the results of ignition test, where a cotton swab soaked with the reference GenF electrolyte quickly catches on fire and burns steadily for nearly 30 seconds. This can be seen to be due to the electrolyte itself burning, as the cotton swab itself remains visually unchanged for the first 15 seconds. By contrast, an identical swab soaked in the IDE/TTE (25/75)/LiFSI electrolyte barely ignites at all. The flame itself is rapidly suppressed, and while the residual heat scorches the cotton, no continuing flammability is seen, indicating IDE/TTE is not only a stable electrolyte for silicon anodes it is also an improvement in cell safety.

Summary

In this paper, we report electrolytes based on the novel lithium-coordinating solvent, isosorbide dimethyl ether (IDE). These electrolytes demonstrate stable cycle life with more than 90% capacity retention on silicon anodes, which is a dramatic improvement over the state-of-the-art carbonate-based electrolyte at 22%. This good cell performance is due to a decreased chemical reactivity of IDE with lithium silicides, which is supported by the minimal organic decomposition seen in the XPS analysis. While IDE was found to have a high stability on its own, it was found that combination with a low-viscosity cosolvent such as TTE can improve discharge capacities without altering the high stability of the IDE. These electrolytes have also been shown to be safe, non-flammable, and IDE is known to be non-toxic and environmentally benign as well. We demonstrated that IDE is an important component of electrolytes which can enable the long-term cycling of silicon-based anode for the next-generation lithium-ion batteries.

Materials and Methods

Electrochemical materials

2032-coin cells were assembled using electrodes made by the Cell Analysis, Modeling, and Prototyping (CAMP) facility at Argonne National Laboratory.

The cathode was made of 90 wt% $LiFePO_4$ (Johnson Matthey, Life Power P2 C-$LiFePO_4$), with 5 wt% C45 carbon black (Timcal) and 5% PVDF binder (Solvey 5130) on a 20 µm aluminum current collector. The total active material loading was 17.73 mg/cm^2. The anode was composed of 80 wt% silicon (Paraclete nSiO), with 10 wt% C45, and 10 wt% partially lithiated polyacrylic acid (PAA) on a 10 µm copper current collector. The total active material loading was 0.88 mg/cm^2. The electrodes were dried under vacuum at 110°C (for cathodes) or 130°C (for anodes) for at least 8 hours before use. All cells contained Celgard 2325 separators and were filled with 40 µL of electrolyte. Battery-grade Gen 2 electrolyte, consisting of 1.2 M $LiPF_6$ in a mixture of ethylene carbonate (EC) and ethyl methyl carbonate (EMC) (3:7 w/w) was provided by Tomiyama Pure Chemical Industries. All solvents were distilled and dried to water content <20 ppm prior to use. Lithium hexafluorophosphate ($LiPF_6$) and lithium bis(fluorosulfonyl)imide (LiFSI) were dried under vacuum prior to use.

Electrochemical characterization

Electrochemical testing was performed on a MACCOR Series 4000 Automated Test System.

For cycle life experiments, cells were initially cycled between 2.7 and 3.35V at a C/20 rate with a 24hr constant voltage hold after three cycles. They were then cycled three times at a C/10 rate, 100 times at a C/3 rate, followed by three times at a C/10 rate. Calendar life experiments followed a previously established protocol, featuring three C/10 cycles, followed by an extended potentiostatic hold at the upper-cutoff voltage (UCV) for 360 hrs.

Electrochemical impedance spectroscopy (EIS) characterization was carried out on a Solartron 1400 CellTest® System. The spectra were recorded in the frequency range from 1MHz to 10 mHz with a 10-

mV applied bias. Experiments were carried out at room temperature, in a coin cell format, with the cells brought to 20% state-of-charge (SOC) based on the discharge capacity of the previous cycle. EIS results are displayed for typical cells, rather than an average.

Material characterization

X-ray photoelectron spectroscopy was performed in a PHI 5000 XPS VersaProbe II system from Physical Electronics. The system is attached to an Ar-atmosphere glovebox and the samples were inserted into the XPS analysis chamber through the glovebox without exposure to air. The spectra were obtained using an Al Kα radiation (hυ = 1486.6 eV) beam (100 μm, 25 W), with Ar^+ and electron beam sample neutralization, in fixed analyzer transmission mode. The base pressure is typically $\sim 2 \times 10^{-8}$ torr or lower in the analysis chamber. To compensate for the effects of surface charging, all core-level spectra were referenced to the C_{1s} hydrocarbon peak at 284.8 eV. Electrodes were rinsed with diethyl carbonate (DEC) before analysis to remove residual solvents and salts.

DFT Calculation

Geometry optimizations and molecular orbital energy calculations were done in the gas phase using the B3LYP hybrid density functional through the GAUSSIAN 09 software package. The 6-311+G(d) basis set was used for all atoms.

Supporting Information

DFT calculations and additional experimental results, including viscosity measurements, flammability tests, extended cycling protocols and supplementary electrochemical data.

Author information

Corresponding author:

Zhengcheng Zhang - *Chemical Sciences and Engineering Division, Argonne National Laboratory, 9700 S. Cass Ave., Lemont, IL 60439, USA; Email: zzhang@anl.gov*

Acknowledgements

Support from Brian Cunningham at Vehicle Technologies Office (VTO), Office of Energy Efficiency and Renewable Energy, U.S. Department of Energy is gratefully acknowledged. LFP cathode and silicon anode were fabricated at Argonne's Cell Analysis, Modeling, and Prototyping (CAMP) Facility. Argonne National Laboratory's work was supported by the U.S. Department of Energy, Office of Energy Efficiency and Renewable Energy (EERE), Office of Vehicle Technologies (VTO), Battery Materials Research (BMR) Program, under contract DE-AC02-06CH11357.

References

1. Choi, N. S.; Chen, Z.; Freunberger, S. A.; Ji, X.; Sun, Y. K.; Amine, K.; Yushin, G.; Nazar, L. F.; Cho, J.; Bruce, P. G., Challenges facing lithium batteries and electrical double-layer capacitors. *Angew Chem Int Ed Engl* **2012,** *51* (40), 9994-10024.
2. Etacheri, V.; Marom, R.; Elazari, R.; Salitra, G.; Aurbach, D., Challenges in the development of advanced Li-ion batteries: a review. *Energy & Environmental Science* **2011,** *4* (9), 3243-3262.
3. Tarascon, J. M.; Armand, M., Issues and challenges facing rechargeable lithium batteries. In *Materials For Sustainable Energy: A Collection of Peer-Reviewed Research and Review Articles from Nature Publishing Group*, World Scientific: 2011; pp 171-179.
4. Wen, C. J.; Huggins, R. A., Chemical diffusion in intermediate phases in the lithium-silicon system. *Journal of Solid State Chemistry* **1981,** *37* (3), 271-278.
5. Obrovac, M. N.; Christensen, L., Structural Changes in Silicon Anodes during Lithium Insertion/Extraction. *Electrochemical and Solid-State Letters* **2004,** *7* (5), A93.
6. Obrovac, M. N.; Krause, L. J., Reversible Cycling of Crystalline Silicon Powder. *Journal of The Electrochemical Society* **2006,** *154* (2), A103.
7. Feng, K.; Li, M.; Liu, W.; Kashkooli, A. G.; Xiao, X.; Cai, M.; Chen, Z., Silicon-Based Anodes for Lithium-Ion Batteries: From Fundamentals to Practical Applications. *Small* **2018,** *14* (8), 1702737.
8. Nesper, R., Structure and chemical bonding in zintl-phases containing lithium. *Prog Solid State Ch* **1990,** *20* (1), 1-45.
9. Key, B.; Bhattacharyya, R.; Morcrette, M.; Seznéc, V.; Tarascon, J.-M.; Grey, C. P., Real-Time NMR Investigations of Structural Changes in Silicon Electrodes for Lithium-Ion Batteries. *Journal of the American Chemical Society* **2009,** *131* (26), 9239-9249.
10. Yoon, T.; Milien, M. S.; Parimalam, B. S.; Lucht, B. L., Thermal Decomposition of the Solid Electrolyte Interphase (SEI) on Silicon Electrodes for Lithium Ion Batteries. *Chemistry of Materials* **2017,** *29* (7), 3237-3245.
11. He, Y.; Jiang, L.; Chen, T.; Xu, Y.; Jia, H.; Yi, R.; Xue, D.; Song, M.; Genc, A.; Bouchet-Marquis, C.; Pullan, L.; Tessner, T.; Yoo, J.; Li, X.; Zhang, J.-G.; Zhang, S.; Wang, C., Progressive growth of the solid–electrolyte interphase towards the Si anode interior causes capacity fading. *Nature Nanotech* **2021,** *16* (10), 1113-1120.

12. Piper, D. M.; Travis, J. J.; Young, M.; Son, S.-B.; Kim, S. C.; Oh, K. H.; George, S. M.; Ban, C.; Lee, S.-H., Reversible High-Capacity Si Nanocomposite Anodes for Lithium-ion Batteries Enabled by Molecular Layer Deposition. *Advanced Materials* **2014,** *26* (10), 1596-1601.
13. Ko, M.; Chae, S.; Ma, J.; Kim, N.; Lee, H.-W.; Cui, Y.; Cho, J., Scalable synthesis of silicon-nanolayer-embedded graphite for high-energy lithium-ion batteries. *Nature Energy* **2016,** *1* (9), 1-8.
14. Jiang, S. S.; Hu, B.; Sahore, R.; Zhang, L. H.; Liu, H. H.; Zhang, L.; Lu, W. Q.; Zhao, B.; Zhang, Z. C., Surface-Functionalized Silicon Nanoparticles as Anode Material for Lithium-Ion Battery. *Acs Applied Materials & Interfaces* **2018,** *10* (51), 44924-44931.
15. Yi, R.; Dai, F.; Gordin, M. L.; Sohn, H.; Wang, D., Influence of Silicon Nanoscale Building Blocks Size and Carbon Coating on the Performance of Micro-Sized Si–C Composite Li-Ion Anodes. *Advanced Energy Materials* **2013,** *3* (11), 1507-1515.
16. Song, J.; Chen, S.; Zhou, M.; Xu, T.; Lv, D.; L. Gordin, M.; Long, T.; Melnyk, M.; Wang, D., Micro-sized silicon–carbon composites composed of carbon-coated sub-10 nm Si primary particles as high-performance anode materials for lithium-ion batteries. *Journal of Materials Chemistry A* **2014,** *2* (5), 1257-1262.
17. Liu, N.; Lu, Z.; Zhao, J.; McDowell, M. T.; Lee, H.-W.; Zhao, W.; Cui, Y., A pomegranate-inspired nanoscale design for large-volume-change lithium battery anodes. *Nature Nanotech* **2014,** *9* (3), 187-192.
18. Chae, S.; Xu, Y.; Yi, R.; Lim, H.-S.; Velickovic, D.; Li, X.; Li, Q.; Wang, C.; Zhang, J.-G., A Micrometer-Sized Silicon/Carbon Composite Anode Synthesized by Impregnation of Petroleum Pitch in Nanoporous Silicon. *Advanced Materials* **2021,** *33* (40), 2103095.
19. Chan, C. K.; Ruffo, R.; Hong, S. S.; Cui, Y., Surface chemistry and morphology of the solid electrolyte interphase on silicon nanowire lithium-ion battery anodes. *Journal of Power Sources* **2009,** *189* (2), 1132-1140.
20. Dalavi, S.; Guduru, P.; Lucht, B. L., Performance Enhancing Electrolyte Additives for Lithium Ion Batteries with Silicon Anodes. *Journal of The Electrochemical Society* **2012,** *159* (5), A642.
21. Xu, C.; Lindgren, F.; Philippe, B.; Gorgoi, M.; Björefors, F.; Edström, K.; Gustafsson, T., Improved Performance of the Silicon Anode for Li-Ion Batteries: Understanding the Surface Modification Mechanism of Fluoroethylene Carbonate as an Effective Electrolyte Additive. *Chemistry of Materials* **2015,** *27* (7), 2591-2599.
22. Choi, N.-S.; Yew, K. H.; Kim, H.; Kim, S.-S.; Choi, W.-U., Surface layer formed on silicon thin-film electrode in lithium bis(oxalato) borate-based electrolyte. *Journal of Power Sources* **2007,** *172* (1), 404-409.
23. Ryu, Y.-G.; Lee, S.; Mah, S.; Lee, D. J.; Kwon, K.; Hwang, S.; Doo, S., Electrochemical Behaviors of Silicon Electrode in Lithium Salt Solution Containing Alkoxy Silane Additives. *Journal of The Electrochemical Society* **2008,** *155* (8), A583.
24. Han, G.-B.; Ryou, M.-H.; Cho, K. Y.; Lee, Y. M.; Park, J.-K., Effect of succinic anhydride as an electrolyte additive on electrochemical characteristics of silicon thin-film electrode. *Journal of Power Sources* **2010,** *195* (11), 3709-3714.
25. Nölle, R.; Achazi, A. J.; Kaghazchi, P.; Winter, M.; Placke, T., Pentafluorophenyl Isocyanate as an Effective Electrolyte Additive for Improved Performance of Silicon-Based Lithium-Ion Full Cells. *ACS Applied Materials & Interfaces* **2018,** *10* (33), 28187-28198.
26. Chen, J.; Fan, X.; Li, Q.; Yang, H.; Khoshi, M. R.; Xu, Y.; Hwang, S.; Chen, L.; Ji, X.; Yang, C.; He, H.; Wang, C.; Garfunkel, E.; Su, D.; Borodin, O.; Wang, C., Electrolyte design for LiF-rich solid–electrolyte interfaces to enable high-performance microsized alloy anodes for batteries. *Nature Energy* **2020,** *5* (5), 386-397.

27. Etacheri, V.; Geiger, U.; Gofer, Y.; Roberts, G. A.; Stefan, I. C.; Fasching, R.; Aurbach, D., Exceptional Electrochemical Performance of Si-Nanowires in 1,3-Dioxolane Solutions: A Surface Chemical Investigation. *Langmuir* **2012,** *28* (14), 6175-6184.
28. Yang, G.; Frisco, S.; Tao, R.; Philip, N.; Bennett, T. H.; Stetson, C.; Zhang, J.-G.; Han, S.-D.; Teeter, G.; Harvey, S. P.; Zhang, Y.; Veith, G. M.; Nanda, J., Robust Solid/Electrolyte Interphase (SEI) Formation on Si Anodes Using Glyme-Based Electrolytes. *ACS Energy Letters* **2021,** *6* (5), 1684-1693.
29. Piper, D. M.; Evans, T.; Leung, K.; Watkins, T.; Olson, J.; Kim, S. C.; Han, S. S.; Bhat, V.; Oh, K. H.; Buttry, D. A., Stable silicon-ionic liquid interface for next-generation lithium-ion batteries. *Nature communications* **2015,** *6* (1), 1-10.
30. Liu, Q.; Jiang, W.; Munoz, M. J. P.; Liu, Y.; Yang, Z.; Bloom, I.; Dzwiniel, T. L.; Li, Y.; Pupek, K. Z.; Zhang, Z., Stabilized Electrode/Electrolyte Interphase by a Saturated Ionic Liquid Electrolyte for High-Voltage NMC532/Si-Graphite Cells. *ACS Applied Materials & Interfaces* **2020,** *12* (20), 23035-23045.
31. Rohrer, J.; Kaghazchi, P., Structure Sensitivity in the Decomposition of Ethylene Carbonate on Si Anodes. *ChemPhysChem* **2014,** *15* (18), 3950-3954.
32. Sprowl, L. H.; Árnadóttir, L.; Chan, M. K. Y., Fluoroethylene Carbonate Breakdown Mechanisms and Energetics on Two Lithium Silicide Surfaces. *The Journal of Physical Chemistry C* **2019,** *123* (44), 26743-26751.
33. Shobukawa, H.; Alvarado, J.; Yang, Y.; Meng, Y. S., Electrochemical performance and interfacial investigation on Si composite anode for lithium ion batteries in full cell. *Journal of Power Sources* **2017,** *359*, 173-181.
34. Jia, H.; Zou, L.; Gao, P.; Cao, X.; Zhao, W.; He, Y.; Engelhard, M. H.; Burton, S. D.; Wang, H.; Ren, X.; Li, Q.; Yi, R.; Zhang, X.; Wang, C.; Xu, Z.; Li, X.; Zhang, J.-G.; Xu, W., High-Performance Silicon Anodes Enabled By Nonflammable Localized High-Concentration Electrolytes. *Advanced Energy Materials* **2019,** *9* (31), 1900784.
35. Harlow, J. E.; Glazier, S. L.; Li, J.; Dahn, J. R., Use of Asymmetric Average Charge- and Average Discharge-Voltages as an Indicator of the Onset of Unwanted Lithium Deposition in Lithium-Ion Cells. *Journal of the Electrochemical Society* **2018,** *165* (16), A3595-A3601.
36. Kalaga, K.; Rodrigues, M.-T. F.; Trask, S. E.; Shkrob, I. A.; Abraham, D. P., Calendar-life versus cycle-life aging of lithium-ion cells with silicon-graphite composite electrodes. *Electrochimica Acta* **2018,** *280*, 221-228.
37. Lu, W.; Zhang, L.; Qin, Y.; Jansen, A., Calendar and Cycle Life of Lithium-Ion Batteries Containing Silicon Monoxide Anode. *Journal of The Electrochemical Society* **2018,** *165* (10), A2179.
38. McBrayer, J. D.; Rodrigues, M.-T. F.; Schulze, M. C.; Abraham, D. P.; Apblett, C. A.; Bloom, I.; Carroll, G. M.; Colclasure, A. M.; Fang, C.; Harrison, K. L.; Liu, G.; Minteer, S. D.; Neale, N. R.; Veith, G. M.; Johnson, C. S.; Vaughey, J. T.; Burrell, A. K.; Cunningham, B., Calendar aging of silicon-containing batteries. *Nature Energy* **2021,** *6* (9), 866-872.
39. Blyth, R. I. R.; Buqa, H.; Netzer, F. P.; Ramsey, M. G.; Besenhard, J. O.; Golob, P.; Winter, M., XPS Studies of Graphite Electrode Materials for Lithium Ion Batteries. *Applied Surface Science* **2000,** *167* (1-2), 99-106.
40. Nguyen, C. C.; Lucht, B. L., Comparative Study of Fluoroethylene Carbonate and Vinylene Carbonate for Silicon Anodes in Lithium Ion Batteries. *Journal of The Electrochemical Society* **2014,** *161* (12), A1933.
41. Doron Aurbach; Idit Weissman, a.; Schechter, A.; Cohen, H., X-ray Photoelectron Spectroscopy Studies of Lithium Surfaces Prepared in Several Important Electrolyte Solutions. A Comparison with Previous Studies by Fourier Transform Infrared Spectroscopy. *ACS Publications* **1996**.
42. Jaumann, T.; Balach, J.; Klose, M.; Oswald, S.; Langklotz, U.; Michaelis, A.; Eckert, J.; Giebeler, L., SEI-component formation on sub 5 nm sized silicon nanoparticles in Li-ion batteries: the role of

electrode preparation, FEC addition and binders. *Physical Chemistry Chemical Physics* **2015,** *17* (38), 24956-24967.
43. Nie, M.; Abraham, D. P.; Chen, Y.; Bose, A.; Lucht, B. L., Silicon Solid Electrolyte Interphase (SEI) of Lithium Ion Battery Characterized by Microscopy and Spectroscopy. *The Journal of Physical Chemistry C* **2013,** *117* (26), 13403-13412.
44. Lin, Y.-X.; Liu, Z.; Leung, K.; Chen, L.-Q.; Lu, P.; Qi, Y., Connecting the irreversible capacity loss in Li-ion batteries with the electronic insulating properties of solid electrolyte interphase (SEI) components. *Journal of Power Sources* **2016,** *309*, 221-230.
45. Han, S.-D.; Wood, K. N.; Stetson, C.; Norman, A. G.; Brumbach, M. T.; Coyle, J.; Xu, Y.; Harvey, S. P.; Teeter, G.; Zakutayev, A.; Burrell, A. K., Intrinsic Properties of Individual Inorganic Silicon–Electrolyte Interphase Constituents. *ACS Applied Materials & Interfaces* **2019,** *11* (50), 46993-47002.

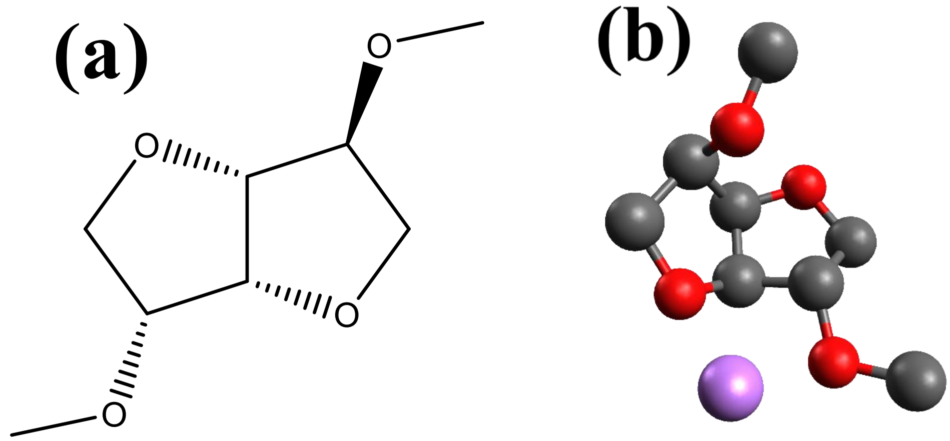

Figure 1. (a) Chemical structure of isosorbide dimethyl ether (IDE) and (b) three-dimensional structure of IDE binding to a lithium ion. Gray = carbon, red = oxygen, purple = lithium. Hydrogen atoms omitted for clarity.

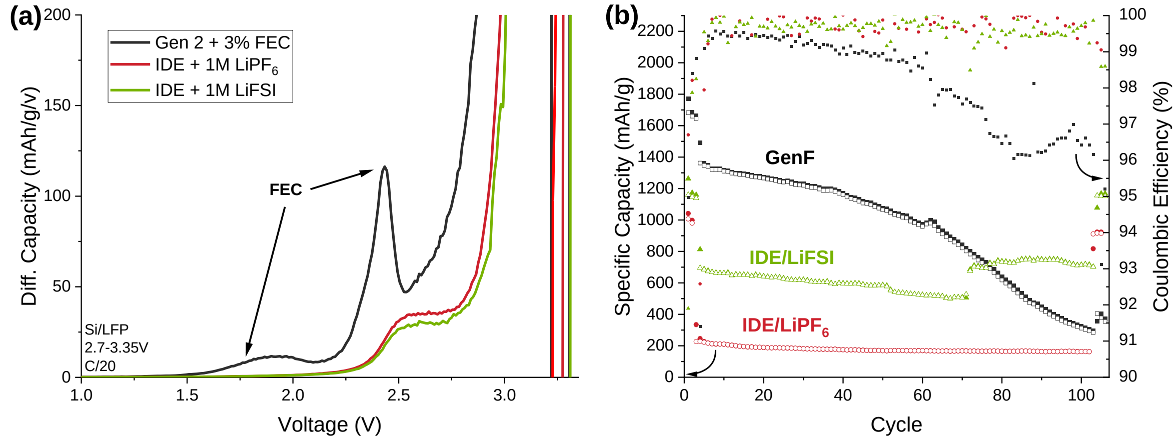

Figure 2. (a) Differential capacity plots of the 1st formation cycle, and (b) specific capacity and Coulombic efficiency of LFP/Si cells containing GenF (1.2 M $LiPF_6$ EC/EMC+3% FEC), 1 M $LiPF_6$ IDE and 1 M LiFSI IDE electrolytes.

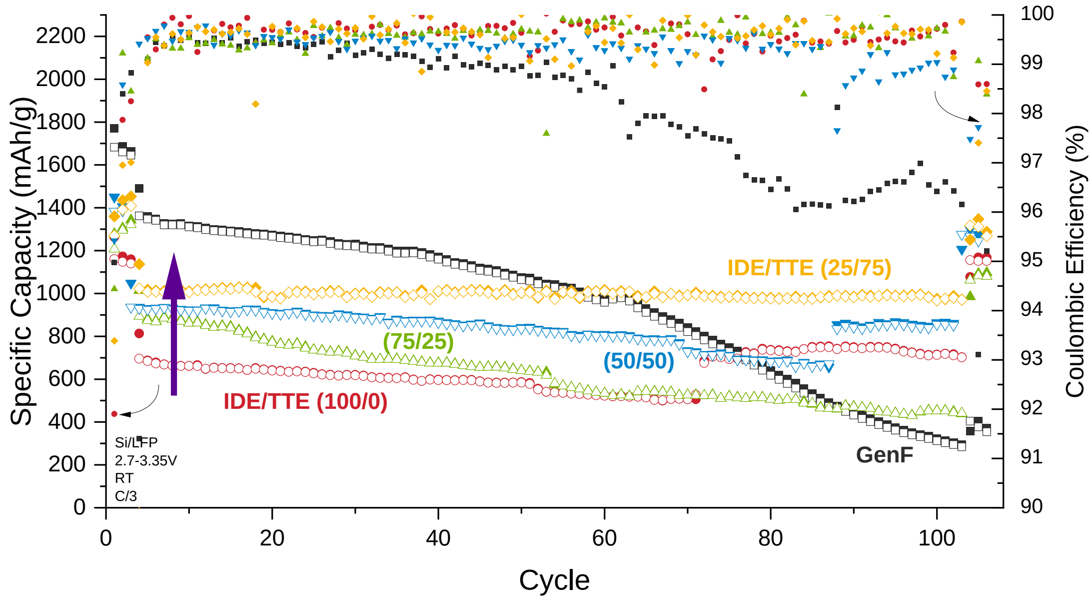

Figure 3. Specific capacity and Coulombic efficiency of LFP/Si cells with IDE/TTE and GenF electrolytes during cycling protocol.

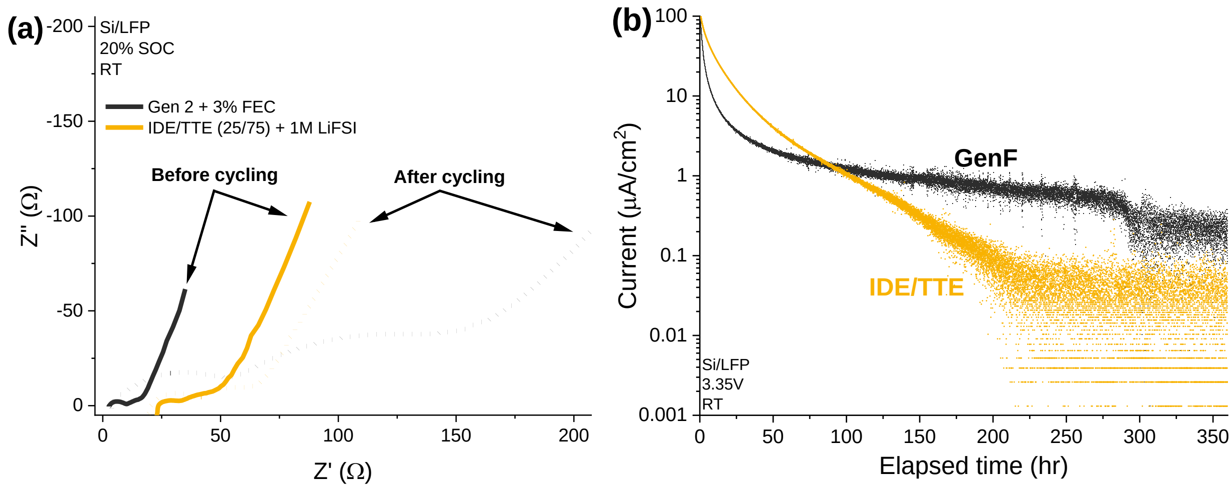

Figure 4. (a) Nyquist plots before and after aging cycles, and (b) leakage current of LFP/Si cells held at a constant potential of 3.35 V using GenF and IDE/TTE electrolytes.

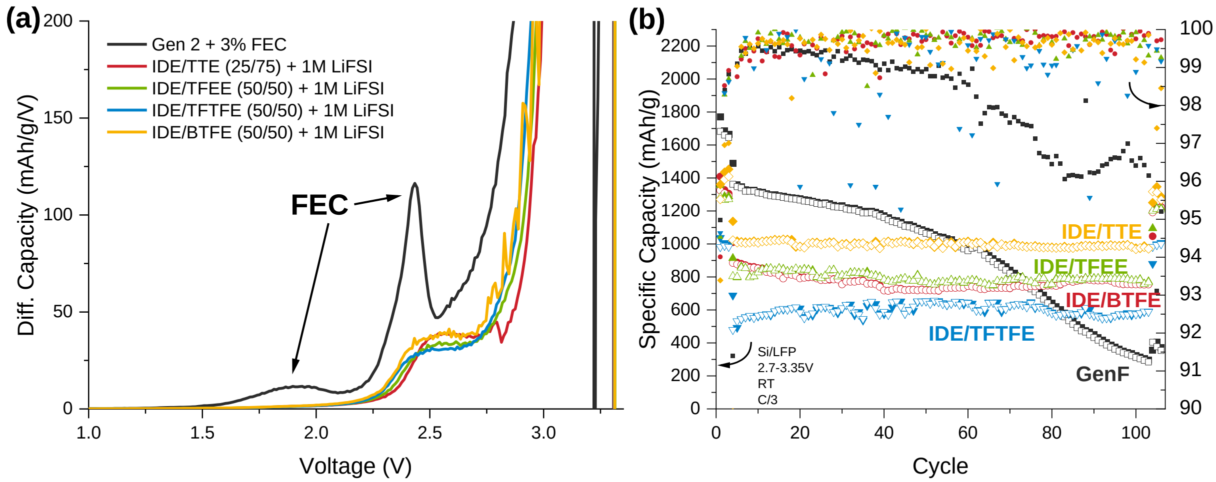

Figure 5. (a) Differential capacity plots and (b) specific capacities and Coulombic efficiencies for IDE/HFE electrolytes compared to GenF.

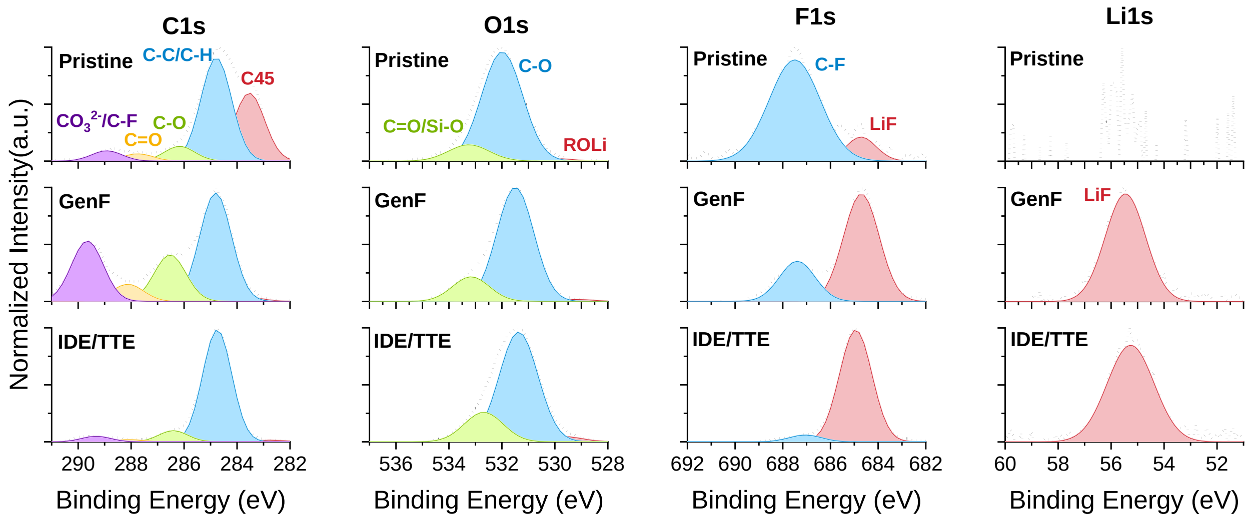

Figure 6. C1s, O1s, F1s and Li1s XPS spectra of pristine and cycled silicon electrodes with GenF and IDE/TTE electrolytes after 100 cycles.